



Validation of a CMOS-MEMS accelerometer based on FGMOS transduction by electromechanical modification of its coupling coefficient

G. S. Abarca-Jiménez¹ · J. Mares-Carreño¹ · M. A. Reyes-Barranca² · B. Granados-Rojas² · S. Mendoza-Acevedo³ · J. E. Munguía-Cervantes³ · M. A. Alemán-Arce³

Received: 17 December 2018 / Accepted: 23 February 2019 / Published online: 29 March 2019

© Springer-Verlag GmbH Germany, part of Springer Nature 2019

Abstract

This paper presents the design and fabrication of an accelerometer prototype through a CMOS silicon foundry with a technology able to deliver a floating-gate MOS transistor (FGMOS). The design of this device included a comb drive capacitor, with aluminum as the structural layer, in order to transform the FGMOS in an inertial sensor and its performance was evaluated electromechanically modifying the coupling coefficient of this FGMOS. A post-process micromachining step was added after the IC chip was received from the foundry. The case here described consists on a surface micromachining step such that the structural layer—aluminum in the case here reported—can be completely released making available a variable coupling capacitor (with air as dielectric) having free movement from which a variable coupling coefficient can be established. The results of a dynamic analysis applied to the resulting CMOS-MEMS structure are shown, demonstrating that this approach is interesting and promisorious as an option for inertial sensors.

1 The FGMOS and its analog applications

FGMOS stands for floating gate (FG) MOSFET or multi input floating gate transistor (MI-FGMOS) in which the threshold voltage can be controlled and tuned through the use of coupling capacitors connected to one or more external control gates, where a bias voltage is applied (Rodríguez-Villegas 2006), as shown in the equivalent electric diagram illustrated in Fig. 1.

Since its appearance, FGMOS transistors have been used mainly in digital circuit designs until quite recently.

Nowadays, this device has been successfully introduced also in analogue applications such as amplifiers and current mirrors (Mejía-Chávez et al. 2011), among others. Besides, it has been reported that the FGMOS transistor is suitable for application as a variable-gain amplifier and some examples are presented in Sharroush (2016) and Lopez-Martinez et al. (2015), as well as in current mirrors Badwal et al. (2014), Sinh and Kumar (2016) and Manhas et al. (2008). All of these designs are exclusively framed within the philosophy of CMOS integrated circuits (IC) design and fabrication, using CMOS-IC silicon foundries. The

✉ J. Mares-Carreño
cmasesj@ipn.mx

G. S. Abarca-Jiménez
gabarcj@ipn.mx

M. A. Reyes-Barranca
mreyes@cinvestav.mx

B. Granados-Rojas
bgranadosr@cinvestav.mx

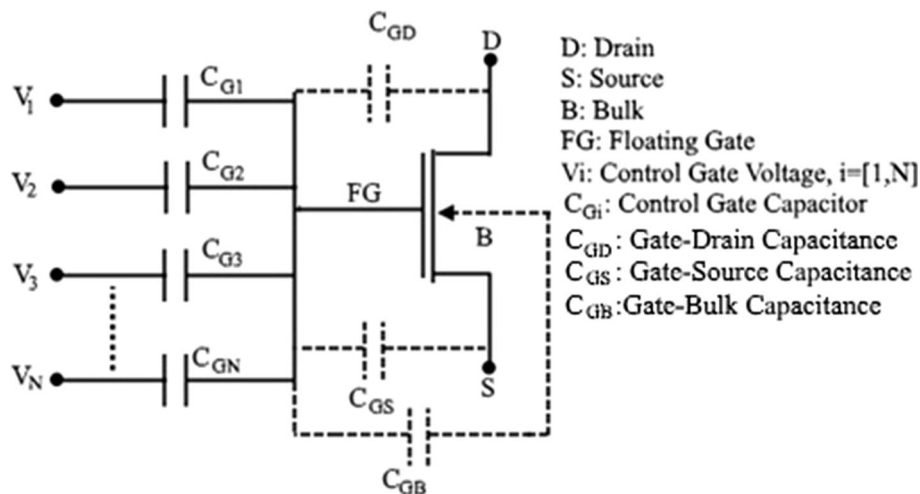
S. Mendoza-Acevedo
smendozaa@ipn.mx

J. E. Munguía-Cervantes
jmunguia@ipn.mx

M. A. Alemán-Arce
maleman@ipn.mx

- ¹ Unidad Profesional Interdisciplinaria de Ingeniería Campus Hidalgo, UPIIH IPN, Boulevard Circuito La Concepción 3, 42162 San Agustín Tlaxiaca, Hidalgo, Mexico
- ² Electrical Engineering Department, CINVESTAV IPN, Av, Instituto Politécnico Nacional 2508, Gustavo A. Madero, San Pedro Zacatenco, 07360 Mexico City, Mexico
- ³ Centro de Nanociencias y Micro y Nano Tecnologías-IPN, Av. Luis Enrique Erro s/n, Nueva Industrial Vallejo, 07738 Mexico City, Mexico

Fig. 1 Schematic representation of the associated capacitances of an n-channel, n-inputs, FGMOS transistor (Abarca-Jiménez et al. 2018)



intention of this work is to show that the capabilities of the FGMOS can be extended beyond these traditional applications, using it as a transducer device in CMOS-MEMS (complementary metal oxide semiconductor-micro electro mechanical systems).

2 CMOS-MEMS to FGMOS-MEMS

The term FGMOS-MEMS is used in this context as a sensor based on a variable coupling coefficient that can be attained thanks to a capacitor located between the control gate and the floating gate with air as dielectric and whose magnitude is modified by mechanical instances. This will place the application of the FGMOS further into the MEMS field, since the variable capacitor needed is constructed making either a bulk or surface micromachining, as is done in MEMS technology. This variation can be achieved since one plate of the capacitor is anchored to the substrate and the other plate is attached to a spring, allowing the separation gap of these plates to be increased or decreased in response to the application of an inertial force. Hence, this can be classified as a CMOS-MEMS monolithic design since associated electronics and MEMS structures can be placed within the same substrate. To accomplish this purpose, a prototype of a single axis accelerometer was selected in order to demonstrate its transducing properties using a relatively simple and easy design keeping in mind that they are commonly used in a huge number of applications (Boser and Howe 1996). In this case we do not present the FGMOS as a variable-gain amplifier, but the main subject of this work is to present a FGMOS as a transducer that can convert a dynamic inertial force into an electrical parameter.

3 Theoretical basis of the prototype proposed

As mentioned above, this work follows the design rules and fabrication steps of a CMOS silicon foundry in order to be able to configure a FGMOS device. The variable capacitor (comb type structure) was included in the same structure, but as this technology does not offer neither bulk or surface micromachining like that offered by MEMS dedicated technologies (like MEMSCAP for instance), a post-process micromachining step is added after the IC chip is received from MOSIS (On Semi's 0.5 μm technology). The case here described consists on a surface micromachining step such that the structural layer—aluminum in the case here reported—can be completely released making available a variable coupling capacitor having free movement establishing a variable coupling coefficient with air as dielectric. The complete micromachining procedure followed to release the structure can be consulted in Abarca-Jiménez (2016). Then, this prototype can be considered as a CMOS-MEMS sensor.

Specifically, the threshold voltage of the FGMOS can be controlled in many ways. This can be achieved featuring either a volatile or non-volatile operation of the FGMOS. Among the volatile operation options, in this work we propose a suitable application where inertial sensing can be established with a mechanically variable capacitor from which control of the sum of the weighted voltage present upon the floating gate can be reached, as the result of applying fixed voltages to the control gates capacitively coupled to the floating gate of the FGMOS. This sum of weighted voltages is induced by the potential applied to the control gate(s) of the transistor via the resultant capacitance voltage divider and it can be calculated by (1) for N control gates:

$$V_{FG} = \sum \alpha_{CGi} V_{CGi} + \frac{C_{GD}}{C_T} V_D + \frac{C_{GS}}{C_T} V_S + \frac{C_{GB}}{C_T} V_B + \frac{Q_{FG}}{C_T}, \tag{1}$$

where:

$$\alpha_{CGi} = \frac{C_{Gi}}{C_T} \text{ with } i = 1, \dots, N, \tag{2}$$

$$C_T = \sum_i C_{Gi} + C_{GD} + C_{GS} + C_{GB}. \tag{3}$$

And C_{Gi} is the capacitance due to each of the N control gates, V_{CGi} is the voltage applied to the i th control gate, C_T is the total equivalent capacitance, V_D is the drain voltage, V_S is the source voltage, V_B is the bulk voltage, C_{GD} is the parasitic overlapping capacitance between the drain and the floating gate, C_{GS} is the parasitic overlapping capacitance between the source and the floating gate, Q_{FG} is any residual charge that may be present on the floating gate, and C_G is defined as the coupling coefficient and is always less than 1. As it is well known, the capacitance value for a parallel-plate capacitor is inversely proportional to the distance between the plates separation, $C' = (\epsilon_0 \epsilon_r)/d$, where C' is capacitance per unit area, ϵ_0 is vacuum permittivity, ϵ_r is dielectric relative permittivity, and d is the distance between capacitor plates. Then, from (1) it is easy to see that any change in α_{CG} will be reflected as a change in the electrical behavior of the FGMOS through V_{FG} , despite the control gate voltage is fixed. V_{FG} can be used instead of V_{GS} in the drain current equation (n-channel FGMOS):

$$I_{DS} = \frac{\mu_n C_{OX} W}{L} \left(V_{FG} - V_{FB} - 2\phi_F - \frac{V_{DS}}{2} \right) V_{DS} \dots - \frac{2}{3} \mu_n \frac{W}{L} \sqrt{2\epsilon_s q N_a} \left((2\phi_F + V_{DB})^{\frac{3}{2}} - (2\phi_F + V_{SB})^{\frac{3}{2}} \right), \tag{4}$$

where μ_n is the carrier mobility, C_{OX} the gate oxide capacitance, W and L the drawn channel width and length of the MOSFET, respectively, V_{FB} the flat-band voltage, $2\phi_F$ is the surface potential, V_{DS} is the drain–source voltage, ϵ_s is the semiconductor permittivity, q is the electron charge, N_a is the substrate impurity concentration, V_{DB} is the drain–bulk voltage and V_{SB} is the source–bulk voltage.

Using (1) and (4) it is possible to establish that there is a way to modulate the drain current in a FGMOS by changing the coupling coefficient although the supply voltages are fixed. In order to verify that this way of changing the current in a FGMOS is possible, an experimental validation was outlined and made.

Using the ON semiconductor 0.5 μm (N-well, double poly, three-metal, $\lambda = 0.3 \mu\text{m}$) technology, six FGMOS transistors with identical geometric features ($W = 20 \lambda$ and $L = 4\lambda$), were designed and fabricated. The six FGMOS are distinguished from each other since each capacitor in the control gate (C_{Gi}) has a different value. Each capacitor (C_{Gi}) is arranged in such a way that the coupling coefficient (C_G) is unique for each one. All transistors include a discharge structure (Rodriguez-Villegas and Barnes 2003) coupled to the floating gate in order to eliminate any charge stored therein due to the manufacturing process. One of the transistors is shown in Fig. 2.

Each capacitor was calculated in such a way that the coupling coefficient varies in ratio, as far as the

Fig. 2 Layout of the FGMOS transistor used to verify the principle of operation

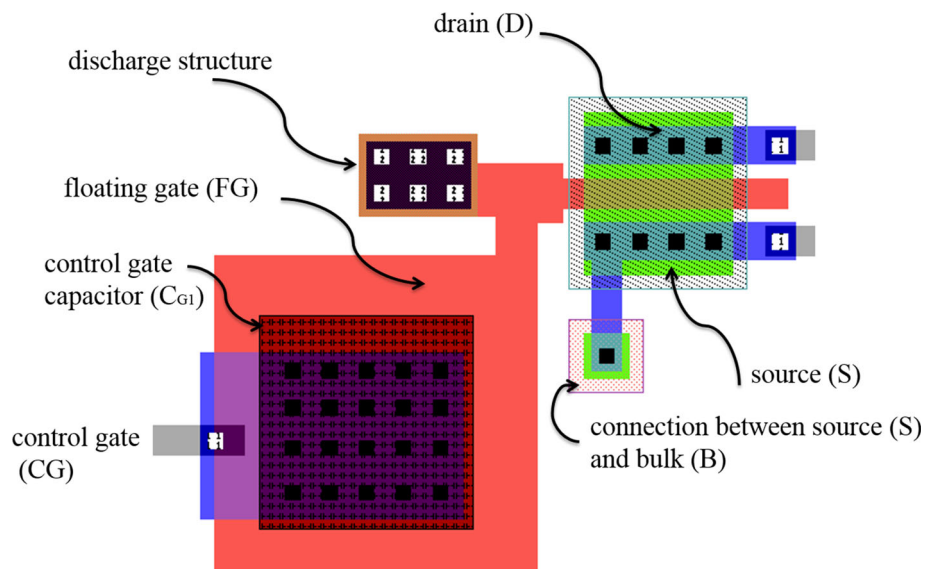


Table 1 Characteristics of the capacitors associated to each coupling coefficient

Transistor	α_{CG}	Capacitor in the control gate (C_{G1}) [F]
FGMOS 6	0.29	5.83×10^{-15}
FGMOS 5	0.36	8.1×10^{-15}
FGMOS 4	0.55	17.03×10^{-15}
FGMOS 3	0.71	34.04×10^{-15}
FGMOS 2	0.79	54.75×10^{-15}
FGMOS 1	0.83	68.12×10^{-15}

technological rules permitted it. The characteristics of each pair capacitor-coupling coefficient are shown in Table 1.

Corresponding experimental output curves of each of the FGMOS described above are shown in Fig. 3. They were obtained using a Keithley 4200A SCS parameter analyzer equipped with I–V source measure units model 4210-SMU. Measurements were made sweeping V_{DS} from 0 to 5 V and fixing the control gate voltage V_{CG} to 5 V.

From Fig. 3 it is possible to conclude that if a fixed operating voltage is set at all control gates of the transistor and if the coupling coefficient is changing somehow, the drain current of the transistor will also change. It is also possible to observe that if the coupling coefficient increases the drain current increases as well; on the other hand, if the coupling coefficient decreases the drain current will follow the same behavior.

With this experiment, we can conclude that the I–V characteristics of the floating gate transistor can be controlled by means of a variable coupling capacitor, this is, a variable coupling coefficient, as predicted by (1). On the other hand, the magnitude, in rest, of the variable capacitor in the gate, has to be carefully chosen since it must be at least of the same order of magnitude of the parasitic

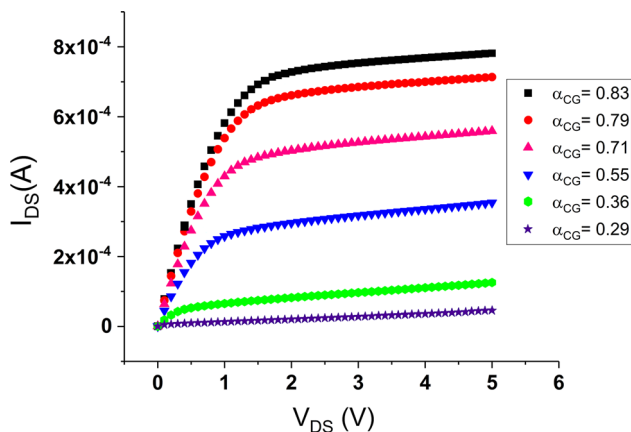


Fig. 3 FGMOS output curves for different coupling coefficient. Using a Keithley 4200A SCS parameter analyzer equipped with I–V Source Measure Units model 4210-SMU FGMOS. Sweeping V_{DS} from 0 to 5 V and fixing the control gate voltage V_{CG} to 5 V

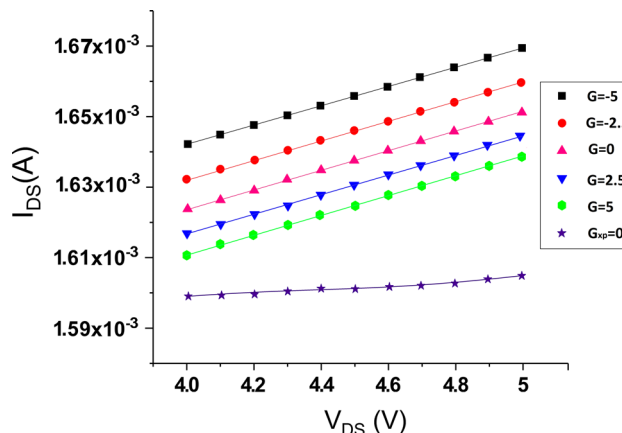


Fig. 4 Current delivered through the FGMOS with different operating voltages and different acceleration values applied

capacitances of the transistor such that the coupling capacitance is not masked by the parasitic capacitances. So there will be the possibility to establish a coupling coefficient value between zero and one due to a mechanical stimulus, allowing the capacitor plates to get close or far each other. Since this mechanism needs movement of the capacitor plates, this can be possible with air as dielectric and this should be considered when the variable capacitance is computed, a fact that will be reflected over the resulting drain current of the FGMOS even when gate and drain bias are fixed.

With the purpose of establishing the range of operation of the transistor, the current delivered through it was obtained. Figure 4 shows the current value with different operating voltages and different acceleration values applied.

From the graph shown in Fig. 4, it is possible to observe that the operating range for the transistor is 4–5 V in V_{DS} , corresponding to a drain current around 1.6 mA. These values were selected in order to establish a range in which the drain current varies as linearly as possible.

4 Variation of the coupling coefficient of FGMOS and integration to an inertial sensor

It should be noted that if it is desired to use the floating gate transistor as a transducer using the control gate capacitor, a coupling coefficient next to zero or one should be avoided. For instance, if the coupling capacitor of the control gate is too small compared to the parasitic capacitances, no matter how much it changes, as long as it remains in the same order of magnitude, it will have no effect on the drain current of the floating gate transistor (Fig. 4), since the coupling coefficient will be very close to zero.

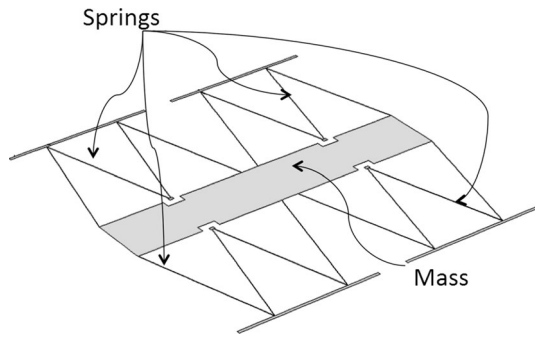


Fig. 5 Mass-spring system

In the opposite case, when the coupling capacitor has a very large magnitude compared to the parasitic capacitances of the transistor, the coupling coefficient will be very close to one and while the capacitor is in that order of magnitude, it will not be possible to control the FGMOS current if slight changes in the capacitor are made.

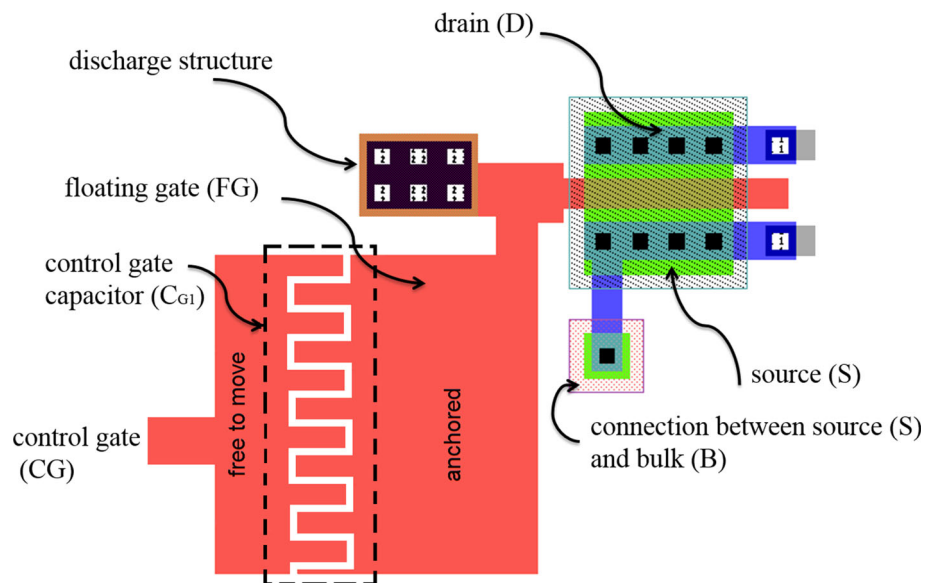
Then, according to the values of coupling coefficient shown in Table 1 and the results shown in Fig. 3, in order to clearly notice a change in the current of the transistor, it would be enough for the capacitor of the control gate to have a variation of about 50% in magnitude.

Looking toward the use of the FGMOS as a transducer, i.e., relating inertial force to drain current, a capacitive microstructure was designed and fabricated.

5 Description of the structure

The proposed structure has the function of replacing the coupling capacitors employed in conventional accelerometers with the FGMOS structure proposed in the previous

Fig. 6 FGMOS transistor used as transducer



experimental section, with a single array of a comb type capacitor with one plate anchored and the other with free movement (mass-spring system, Fig. 5), as is shown in Fig. 6. Thus, when an inertial force is experienced, the capacitive structure under this force will have a capacitance magnitude associated with a specific magnitude of inertial force due to the resulting displacement of the parallel plates, and at the same time, this is traduced into a specific current delivered by the associated FGMOS.

The capacitive structure was designed such that it has a variation of the capacitance value due to increasing or decreasing the separation of the capacitor electrodes as an inertial force is applied. Thus a fixed electrode is anchored to the substrate and the second electrode is formed by a mass-spring system that will help to displacement when the proof mass experiences an inertial force as it is shown in Abarca-Jiménez et al. (2015). The aspect ratio of the integrated FGMOS transistor is $W/L = 20 \lambda/4 \lambda$.

The capacitive structure was calculated, simulated and fabricated with the following characteristics: the two inner metal layers (named metal 1 and metal 2 in the 0.5 μm on-semi technology) were used as structural layers. These two metal layers are joined by a via layer; the structure is designed for a maximum displacement of 0.3 μm when it experiences an acceleration of 6G, for smaller accelerations the proof mass will have smaller displacement following the Hook's law.

6 Post-processing with Silox Vapox II

The complete system was fabricated using the 0.5 μm on-semi technology in a monolithic integration presentation and was encapsulated in a ceramic DIP40 package with

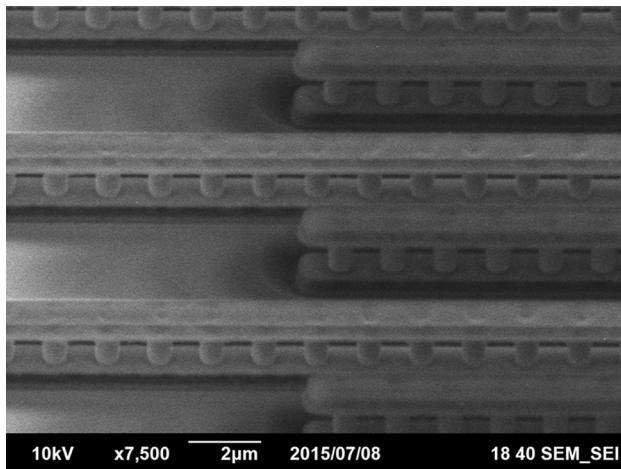


Fig. 7 Capacitive structure fabricated and released after a post-processing surface micromachining. Detail shown in the SEM photograph corresponds to the comb-type capacitor structure

lids. A micromachining post-process was required in order to release one of the electrodes of the capacitive structure from the sacrificial layer (SiO_2). A SEM photograph of the capacitive comb type structure fabricated and already released can be seen in Fig. 7.

Here it can be seen the fingers of the structure perfectly released after the micromachining post-process, as reported in Abarca-Jiménez (2016). Once released, the chip was mounted for measurement as described in the next section.

7 Assembly for experimental test

The experimental results were obtained with a custom fabricated set-up. It consists on a centrifuge and a data acquisition interface using a National Instruments DAQ for data acquisition and a proprietary template made in LabVIEW for data processing. The centrifuge has a user interface that allows establishing an acceleration ramp, which can only be configured for positive accelerations with a maximum value of 16 G.

The prototype MEMS sensor was placed on the centrifuge together with a reference sensor (MPU6050 from InvenSense Inc.) in order to be able to compare the performance of both signals, see Fig. 8.

After measuring the prototype, a relationship of capacitance as a function of displacement of the capacitor plates of the capacitive structure designed was obtained, using Newton's second law and Hooks Law. From this, the amount of displacement of the capacitive structure corresponding to an amount of capacitance in the floating gate can be correlated to the amount of current delivered by the FGMOS, as well. Finally, using a current to voltage converter included within the set-up, the data is processed in

the data acquisition interface. Then, current or voltage readings can be used for correlating the inertial stimulus into an electrical parameter.

8 Results and data analysis

The reference accelerometer used in this test is MPU6050 from InvenSense Inc. which has a digital-output triple-axis accelerometer with a programmable full scale range of $\pm 2 g$, $\pm 4 g$, $\pm 8 g$ and $\pm 16 g$ and for this the characterization it was programmed for this last acceleration range. The output of this device is transmitted by a digital wireless interface and the acceleration values were obtained and converted regarding the sensitivity at which the sensor was configured. Finally, data was obtained as a function of the angular velocity of the centrifuge vs the acceleration registered by the sensor, see Fig. 9.

Voltage output obtained from the reference device as well as from the prototype was processed with the data acquisition interface in order to relate acceleration in G's with angular velocity, in revolutions per minute (RPM). This can be done with Eq. (5):

$$a = r \times \omega^2 \quad (5)$$

with

$$\omega = 2\pi f \quad (6)$$

where a is the acceleration in (m/s^2), r is the radius (distance from the center of the centrifuge to the device) in (m), ω is the angular velocity (RPM), and f is the frequency (1/s).

Equation (5) represents a parabola and it can be seen in Fig. 9 that experimental data obtained for the prototype designed (box markers) fits rather well with the analytical model (dashed line) almost all over the angular velocity range used. On the other side, experimental data obtained from the reference device (triangle markers) follows the model faithfully (dots line) only when $\omega > 180$ RPMs. This may be caused since the reference accelerometer was programmed for the higher acceleration range ($\pm 16 G$'s) and maybe there can be some deviation at acceleration values $< 2 G$'s. However, Fig. 9 is a confirmation that the approach here presented can be feasible and it proves that an accelerometer based on a standard CMOS technology with a FGMOS used for transduction can be achieved. This gives an alternate transduction method, different from those commonly used.

To determine the quality and performance of a sensor it is common to analyze the sensitivity of it. For the case of digital sensor MPU6050, when it is set to full scale ($\pm 16 G$, in this case), the sensitivity is 2048 LSB/G. Highlighting that this value is constant for all this

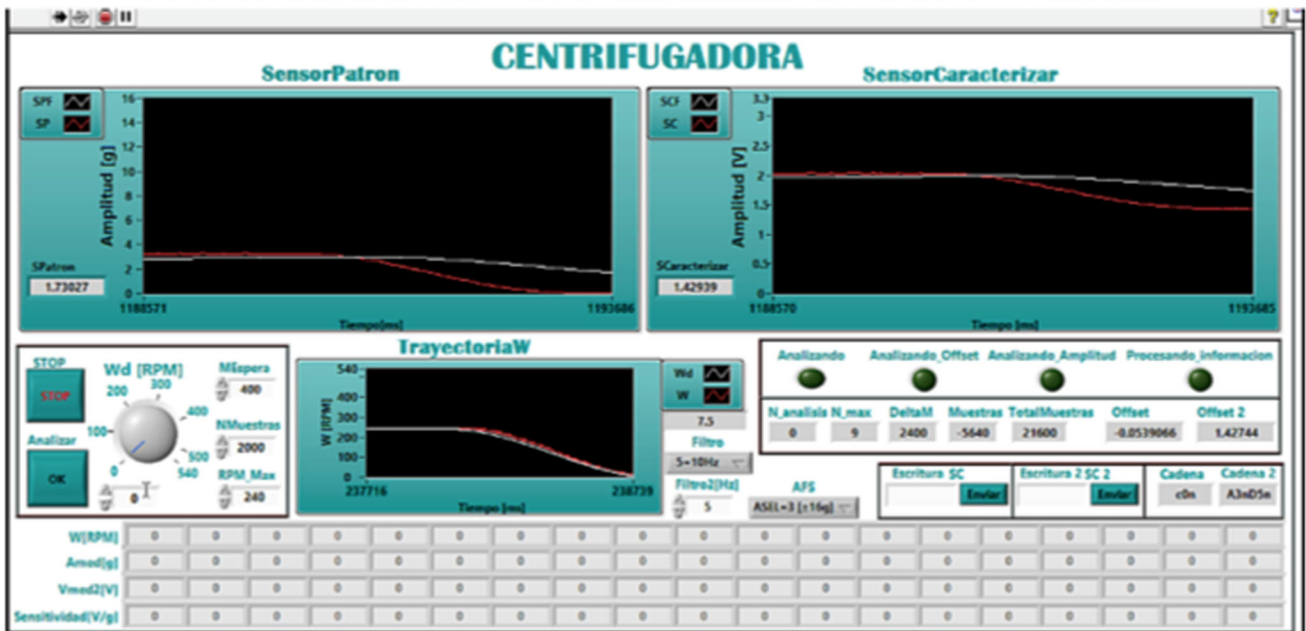
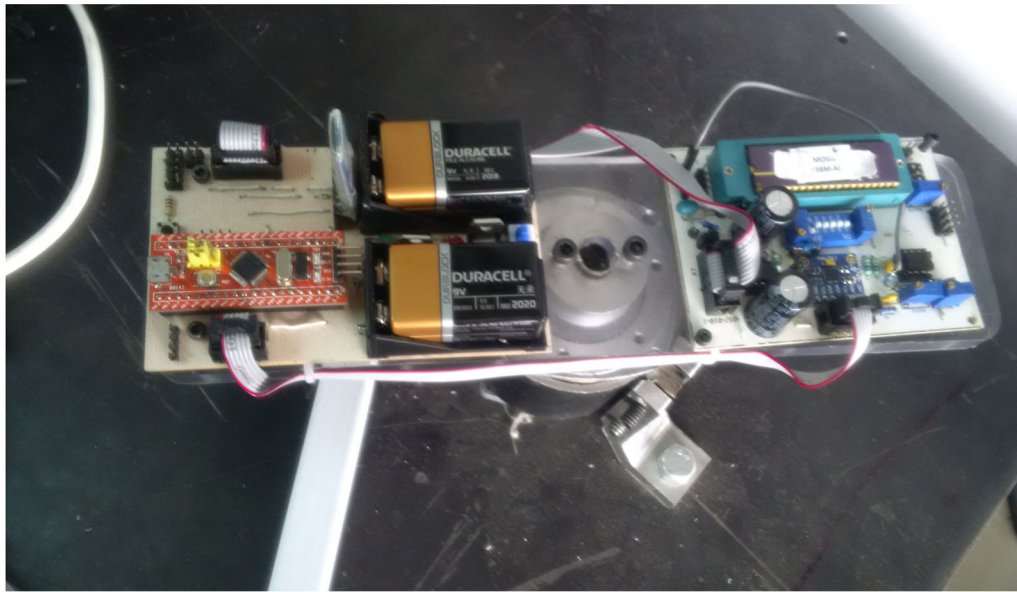


Fig. 8 Centrifuge and data processing unit. It shows how the sensors were mounted and moved to measure performance of reference and proposed prototype

acceleration range, since this sensor is precalibrated. The sensitivity of the sensor presented here is obtained by dividing the voltage value that is read from the data acquisition system with respect to the acceleration that the centrifuge applies to the MEMS sensor. The data acquisition system transforms the variable output current of the FG MOS into an output voltage and then this data is digitized to display it on the screen (Fig. 8). The ratio between voltages delivered by the data acquisition system with the applied acceleration determines the sensitivity of our sensor, which is approximately 15 mV/G, see Fig. 10.

Note from Fig. 10 that the sensitivity of the MEMS sensor is not constant; this was expected due to the variation of the current in the sensor with respect to the variation in the coupling coefficient. This is an issue that deserves further study.

In Fig. 11 a theoretical analysis of the relation between the linear variation of the variable coupling coefficient and the drain current is presented. Note that although the capacitance varies linearly with respect to the displacement of the mass, because of the relation between the coupling coefficient and the drain current, the variation of the sensor will not be linear.

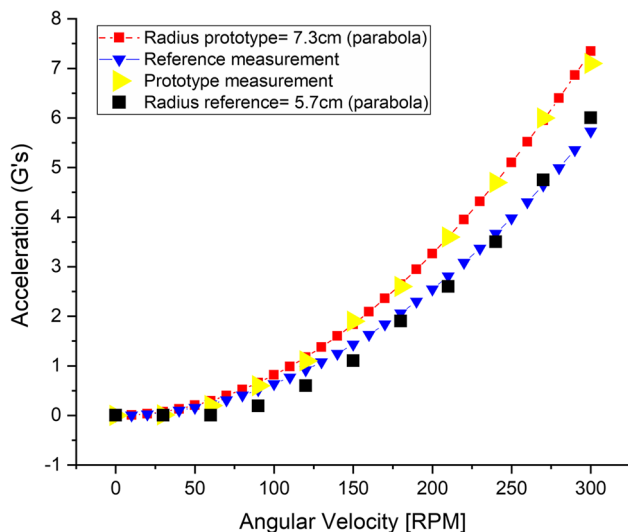


Fig. 9 Experimental results of a dynamic acceleration measurement. Angular velocity of the centrifuge vs the acceleration registered by the sensor. Figure inset shows the radius of the position where each device is located over the centrifuge arm (see Fig. 8)

9 Discussion

Since the purpose of this proposal is to present a new approach from where an accelerometer can be fabricated using a FGMOS as the transducing element based on an affordable technology as that offered by MOSIS, like the CMOS technology of on semi ($0.5\ \mu\text{m}$, triple metal, double poly), some issues related to the development of this device are presented.

First of all, it is experimentally demonstrated that a parallel plate variable capacitor can be configured with a comb type array with a stack of two metal layers. One plate of this array is anchored and taking the role of a control

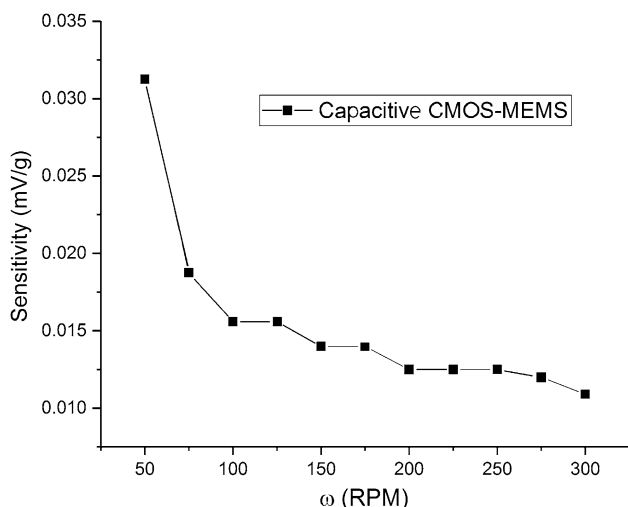


Fig. 10 Sensitivity curve for the capacitive CMOS_MEMS sensor. V_{DS} set at 2.8 V and V_{CG} set at 2.8 V

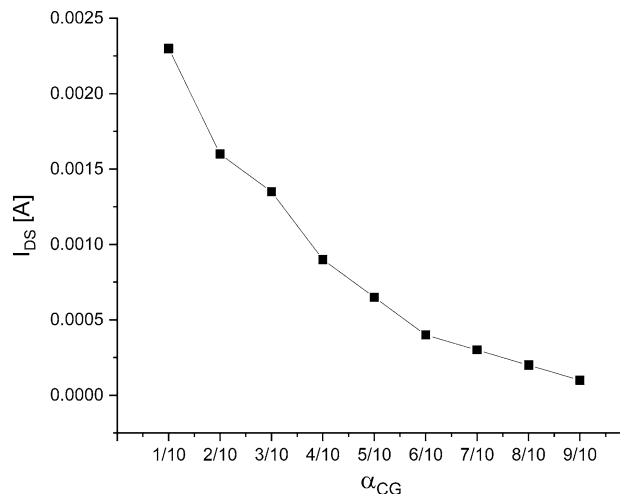


Fig. 11 Coupling coefficient vs drain current. With V_{DS} set at 4 V and V_{CG} set at 5 V

gate. If the other plate of this parallel plate capacitor is released, it should be able to move responding to a force applied externally, taking at the same time the role of floating gate of the FGMOS. If this is possible, one can recall the concept of couple coefficient typically applied to FGMOS devices from its equivalent capacitance model, resulting in drain current modulation. As it is well known, this can be done with methods already demonstrated and commonly used, like Fowler–Nordheim tunneling (FNT) or channel hot electrons (CHE), which are based on electric fields derived from applied voltages. However, if the distance between plates of a capacitor can change, the coupling coefficient can be changed as well, but with mechanical instances.

The study delineated in Sect. 6 shows how a surface micromachining step can be done to the prototype presented, in order to release the capacitor structure that is made part of a FGMOS as described above. As mentioned before, this was applied to an integrated circuit fabricated with a standard CMOS technology with a micromachining post-process through pad windows opened in the protection overglass only where the proof mass of the structure is placed. It should be mentioned that this micromachining step was done over an encapsulated chip placing a single drop of the pad etcher used (Silox-Vapox from Transene) that covered just the area of the chip.

A custom made setup was used for characterization of the structure with a centrifuge that can give a maximum acceleration of 16 G's. Although lateral surface of the parallel plate capacitor is not completely solid, as it is in accelerometers made with dedicated technologies as PolyMUMPS or MetalMUMPS, it was demonstrated that the proposed device responds quite well compared with a reference commercial accelerometer. Then, it is

demonstrated that the coupling coefficient can be modified mechanically, giving a different approach from that used in conventional accelerometers, which use sensing based on differential capacitances.

From Fig. 9 it is possible to highlight some important points. The shape of both curves is highly similar, since both curves can be represented by a polynomial of degree two. Using a curve-fitting method it is possible to affirm that the curve of the experimental results for the case of the standard sensor can be described with the equation $f(x) = 8.47 \times 10^{-5}x^2 - 0.0054x$ and for the case of the MEMS sensor the corresponding equation is $f(x) = 7.70 \times 10^{-5}x^2 - 0.0011x$, in a range of 0–300 rpm. Therefore, it is possible to emphasize that even when our MEMS sensor is not calibrated, the measurement resulted in the expected trace, represented by a parabola. It is also possible to highlight that because the MEMS sensor does not have a constant sensitivity value, a characterization and calibration is required for its use.

The proposal here presented is an initial study and it is obvious that there is still a lot of work to be done to optimize the micromachining post-process and the structure design with a FGMOS embedded as the transducing element so as to have good performance. Meanwhile, it was important to demonstrate that the features of the FGMOS can be extended beyond those already demonstrated and used, mainly based on electric fields. Besides, this study is an option that can be developed using a standard CMOS technology that can be extended to a CMOS MEMS technology with a surface micromachining post process.

10 Conclusions

A structure was proposed as an inertial sensor that demonstrates that the coupling coefficient associated with a FGMOS can be modified mechanically allowing drain current modulation. This mechanism can be used as a transduction principle applied to an inertial sensor as an accelerometer. A standard CMOS technology was used to fabricate an accelerometer prototype and a simple surface micromachining step was added after reception of chips, framing this design into a CMOS-MEMS device. Although it is clear that there are some technical and operating disadvantages with this initial design, it is clear that a system can be configured in the same substrate with non-

proprietary technology. Work is still being made in order to optimize this design, together with some other MEMS devices that can extend the use of FGMOS devices, apart from those normally used for drain current modulation.

Acknowledgements The authors acknowledge SIP-IPN (Grants 20180550, 20180782, 20195839 and 20196281) and Unidad Profesional Interdisciplinaria de Ingeniería Campus Hidalgo-Instituto Politécnico Nacional for their support.

References

- Abarca-Jiménez GS (2016) Ph. D. dissertation Sistema electrónico para un acelerómetro empleando un FGMOS para correlación de parámetro inercial, CINVESTAV-IPN, Mexico
- Abarca-Jiménez GS, Reyes-Barranca MA, Mendoza-Acevedo S (2015) Design consideration and electro-mechanical simulation of an inertial sensor based on a floating gate metal-oxide semiconductor field-effect transistor as transducer. *Microsyst Technol* 21(3):1353–1362
- Abarca-Jiménez GS, Mares-Carreño J, Reyes-Barranca MA, Granados-Rojas B, Mendoza-Acevedo S, Munguía-Cervantes JE, Alemán-Arce MA (2018) Inertial sensing MEMS device using a floating-gate MOS transistor as transducer by means of modifying the capacitance associated to the floating gate. *Microsyst Technol* 24:2753–2764
- Badwal D, Kaur J, Chaudhary SR (2014) FGMOS based current mirror. *Int J Adv Res Comput Sci Softw Eng* 4(8):155–159
- Boser BE, Howe R (1996) Surface micromachined accelerometers. *IEEE J Solid Stated Circ* 31(3):366–375
- Lopez-Martinez NG, Medina-Vazquez AS, Gurrola-Navarro MA (2015) Experimental analysis of a transconductor-amplifier based on a mi-fgmos transistor. In: 12th international conference on electrical engineering, computer science and automatic control (CCE)
- Manhas PS, Sharma S, Pal K, Margotra LK, Jamwal KKS (2008) High performance FGMOS-based low voltage current mirror. *Indian J Pure Appl Phys* 46:355–358
- Mejía-Chávez P, Sánchez-García JC, Velázquez-López J (2011) Differential difference amplifier FGMOS for electrocardiogram. In: International conference on electrical engineering computing science and automatic control
- Rodriguez-Villegas E (2006) Low power and low voltage circuit design with the FGMOS transistor. In: *IET circuits, devices & systems*, vol 20
- Rodriguez-Villegas E, Barnes H (2003) Solution to trapped charge in FGMOS transistors. *Electron Lett* 39(19):1416–1417
- Sharroush SM (2016) A novel variable-gain amplifier based on an FGMOS transistor. In: 5th international conference on electronic devices, systems and applications (ICEDSA), vol 3, no 16
- Sinh N, Kumar H (2016) Low voltage FGMOS based current mirror. *Int J Sci Eng Technol Res (IJSETR)* 5(9):2840–2843

Publisher's Note Springer Nature remains neutral with regard to jurisdictional claims in published maps and institutional affiliations.